

Journal of Medicinal Chemistry

© Copyright 2001 by the American Chemical Society

Volume 44, Number 6

March 15, 2001

Expedited Articles

A Novel Series of Highly Potent Benzimidazole-Based Microsomal Triglyceride Transfer Protein Inhibitors

Jeffrey A. Robl,* Richard Sulsky, Chong-Qing Sun, Ligaya M. Simpkins, Tammy Wang, John K. Dickson, Jr., Ying Chen, David R. Magnin, Prakash Taunk, William A. Slusarchyk, Scott A. Biller, Shih-Jung Lan, Fergal Connolly, Lori K. Kunselman, Talal Sabrah, Haris Jamil, David Gordon, Thomas W. Harrity, and John R. Wetterau

The Bristol-Myers Squibb Pharmaceutical Research Institute, P.O. Box 5400, Princeton, New Jersey 08543-5400

Received November 21, 2000

A series of benzimidazole-based analogues of the potent MTP inhibitor BMS-201038 were discovered. Incorporation of an unsubstituted benzimidazole moiety in place of a piperidine group afforded potent inhibitors of MTP in vitro which were weakly active in vivo. Appropriate substitution on the benzimidazole ring, especially with small alkyl groups, led to dramatic increases in potency, both in a cellular assay of apoB secretion and especially in animal models of cholesterol lowering. The most potent in this series, **3g** (BMS-212122), was significantly more potent than BMS-201038 in reducing plasma lipids (cholesterol, VLDL/LDL, TG) in both hamsters and cynomolgus monkeys.

Introduction

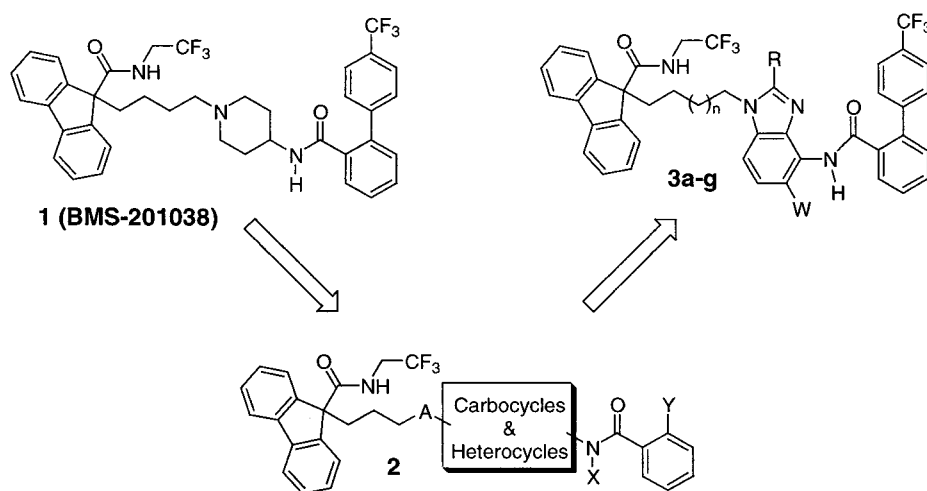
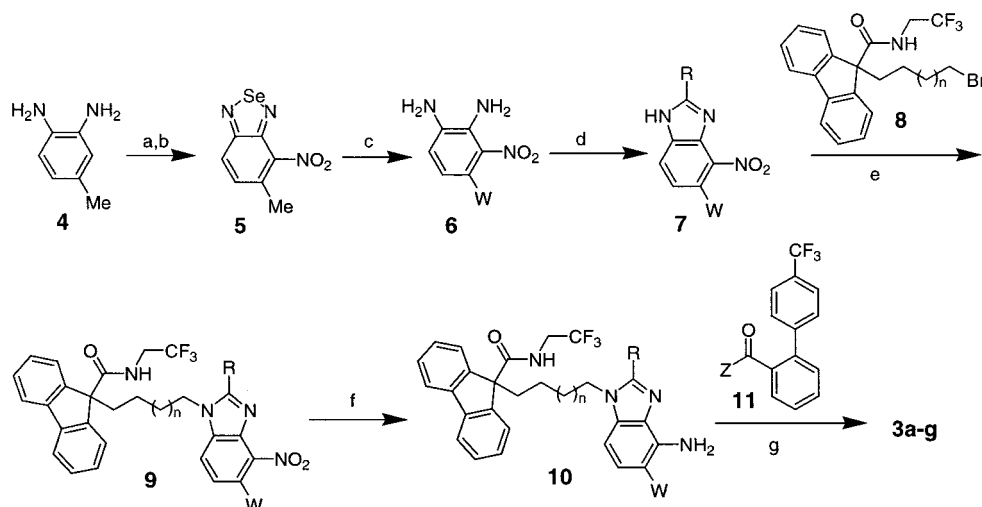
Despite major advances in pharmaceutical and surgical treatments, coronary heart disease (CHD) remains the major cause of death in the industrialized world.^{1,2} Elevated LDL cholesterol has been identified as a key risk factor for CHD, and statin therapy for hypercholesterolemia has been shown to lower the risk for CHD by approximately one-third.³ It remains to be determined whether more aggressive LDL-lowering therapy, or impact on related lipid risk factors such as elevated triglycerides and low HDL, can lead to further reductions in CHD risk. Currently, there has been an increased focus on the treatment of concomitant hypertriglyceridemia, and statins generally have a modest impact on triglyceride levels.

Microsomal triglyceride transfer protein (MTP) is a key factor in the assembly of VLDL, the direct precursor to LDL.⁴ In a recent publication, we outlined the design

and pharmacology of BMS-201038 (**1**), a potent inhibitor of MTP, and described its robust efficacy in lowering plasma cholesterol and triglycerides in both Golden Syrian hamsters and WHHL rabbits.⁵ Based on its efficacy and safety profile, BMS-201038 was advanced into clinical trials. Our focus was subsequently directed toward the identification of a suitable back-up clinical candidate to BMS-201038. A substantial amount of structure–activity studies (SAR) were performed incorporating various carbocycles and heterocycles, generically depicted by structure **2** (Chart 1), as replacements for the piperidine ring in BMS-201038. A driving force for this change was a concern with the ubiquitous presence of piperidine pharmacophores in ligands for G-protein coupled receptors. Within the chemical program, particular emphasis was placed on the incorporation of basic functionalities which would aid in the solubility of these rather lipophilic molecules. Heteroaryl scaffolds were particularly attractive since additional substituents could readily be built upon these cores. Approximately 20 piperidine replacements were

* To whom correspondence should be addressed. Tel: (609) 818-5048. Fax: (609) 818-3550. E-mail: Jeffrey.Robl@bms.com.

Chart 1

Scheme 1^a

^a (a) SeO_2 , 2.4 N HCl, 80 °C (95%); (b) HNO_3 , H_2SO_4 , 10 °C (91%); (c) 57% HI, 50 °C (88%); (d) 2,4-pentanedione, 5 N HCl, EtOH, reflux, 1 h (R = Me, 98%); 98% HCO_2H , reflux (R = H, 95–97%); $n\text{-C}_3\text{H}_7\text{C(OMe)}_3$, PPTS, dioxane, reflux (R = $n\text{-Pr}$, 77%); $i\text{-C}_3\text{H}_7\text{CO}_2\text{H}$, 4 N HCl, reflux (R = $i\text{-Pr}$, 100%); (e) K_2CO_3 , DMF, rt; (f) H_2 , Pd/C, EtOH, rt; (g) EDAC, TEA, CH_2Cl_2 , rt (when Z = OH) or TEA, CH_2Cl_2 , 0 °C (when Z = Cl).

explored in addition to changes within the linker group (A) and the terminal amide functionality. This manuscript highlights *in vitro* and *in vivo* SARs of a select group of compounds which incorporate a benzimidazole core as the central heteroaryl ring, resulting in an exceptionally potent series of novel MTP inhibitors.

Chemistry

Generation of the benzimidazole precursors and incorporation within the BMS-201038 scaffold are depicted in Scheme 1. In the case where W is hydrogen, the nitrodiamine 6 was obtained commercially. Where W was methyl, the requisite nitrodiamines were prepared following the procedures described by Grivas et al.⁶ For example, treatment of 4 with SeO_2 in 3 N HCl afforded the corresponding selenocycle which underwent nitration to afford regioisomer 5 exclusively in good overall yield. Conversion to the diamine 6 (W = Me) was effected by treatment with HI in concentrated HCl. Functionalized nitrobenzimidazoles 7 were easily prepared from the corresponding nitrodiamines 6 exploiting several methodologies: either by reacting the diamines

with the corresponding acid under acidic conditions (as with formic or isobutyric when R = H or $i\text{-Pr}$, respectively), by reaction with an orthoacetal (as when R = Pr), or by reaction with 2,4-pentanedione (as when R = Me). Alkylation of 7 with fluorenylamide 8 (readily prepared in two steps from 9-fluorenylcarboxylic acid) in DMF with K_2CO_3 as base often provided mixtures of regioisomers (e.g. 3.2:1 when R = H, 7:1 when R = Me) which could be readily separated by flash chromatography. In all cases, and especially with alkyl substituents at R, the desired alkylation regioisomer 9 (as shown) was the predominant product. Simple catalytic hydrogenation provided amines 10 which were subsequently acylated with 4'-(trifluoromethyl)-2-biphenylcarboxylic acid via EDAC activation or by reaction with the corresponding acyl chloride to afford the final products 3a–g.

Results and Discussion

A comparison of these compounds shows that potency *in vitro*, and especially *in vivo*, was critically dependent on both the length of the alkyl chain joining the fluo-

Table 1. Inhibition of MTP in Vitro and the in Vivo Efficacy Responses in Lowering TC in Hamsters and Cynomolgus Monkeys for Compounds **1** and **3a–g**

compd ^a	<i>n</i>	R	W	MTP TG transfer assay: IC ₅₀ (nM) ^b	apoB secretion HepG2 cells: IC ₅₀ (nM) ^b	TC lowering in hamsters: % @ mg/kg or ED ₅₀ (mg/kg) ^c	TC lowering in monkeys: % @ mg/kg or ED ₅₀ (mg/kg) ^d
1				8	0.8	2.3	–88% @ 10 –74% @ 5 –65% @ 2.5 –35% @ 1.25 ED ₅₀ = 2 mg/kg nd
3a	0	H	H	10	nd ^e	–11% @ 15	–52% @ 5 –19% @ 2.5
3b	1	H	H	5	0.24	12	–68% @ 2.5 –80% @ 5 –51% @ 1.25
3c	1	H	Me	1	0.02	3.8	–39% @ 2.5
3d	1	Me	H	1	0.15	2.5	–83% @ 1.25 –76% @ 1 –43% @ 0.3 –28% @ 0.1 ED ₅₀ = 0.38 mg/kg
3e	1	<i>i</i> -Pr	H	4	0.06	–60% @ 8	
3f	1	<i>n</i> -Pr	H	2	nd	–44% @ 15	
3g	1	Me	Me	1	0.03	0.28	

^a All spectral data were consistent with the assigned structures. ^b The TG transfer and apoB secretion assays were performed as described in ref 6. ^c ED₅₀ represents dose (mg/kg) required for 50% lowering of plasma TC in standard-diet-fed Golden Syrian hamsters 16 h postdosing or percent TC lowering at dose (mg/kg) (compound administered once daily orally for 3 days). ^d ED₅₀ represents dose (mg/kg) required for 50% lowering of plasma TC in standard-diet-fed cynomolgus monkeys 16 h postdosing or percent TC lowering at dose (mg/kg) (compound administered once daily orally for 7 days). ^e nd, not determined.

renylbenzimidazole moieties as well as the substituents on the benzimidazole ring (Table 1). Compounds were evaluated for inhibition of human MTP activity in vitro (triglyceride transfer assay) and in HepG2 cells (apoB secretion assay). In vivo activity was determined in both hamsters (3 days, po, qd, standard diet) and cynomolgus monkeys (7 days, po, qd, standard diet) as compared to the clinical agent BMS-201038 (**1**). Direct replacement of the piperidine moiety in **1** with an unsubstituted benzimidazole group, affording **3b**, resulted in a slight enhancement of in vitro activity in both the triglyceride transfer and HepG2 apoB secretion assays. Unfortunately, this modification attenuated the ability of **3b** to lower cholesterol in both the rodent and primate models. Shortening the linker group to three carbons to afford **3a** essentially abolished activity in the hamster, despite reasonable activity in the transfer assay. Significant enhancements in potency were realized by incorporation of small substituents at the R and/or W positions of the benzimidazole ring. Due to sensitivity limitations of the transfer assay, the secretion assay was primarily utilized to differentiate among the most potent compounds (**3c–g**). Compounds **3c–g** were 5–40-fold more active than **1** in the apoB secretion assay, which on the basis of our experience usually translates to greater potency in vivo. Although larger alkyl substituents at R (isopropyl and *n*-propyl, **3e,f**, respectively) diminished cholesterol lowering in the hamster and monkey as compared to piperidine **1**, substitution with methyl (**3d**) significantly enhanced in vivo potency as compared to **3b**. A similar boost in potency was observed by the addition of methyl at W (**3c**). Remarkably, incorporation of methyls at both R and W to give **3g** resulted in a synergistic effect in vivo, affording a 43- and 13-fold enhancement in potency in the hamster and monkey, respectively, over **3b**.

The significant potency of **3g** in these models warranted detailed evaluation of this compound in vivo. The dose–response for **3g** upon 3-day treatment in standard chow-fed hamsters (oral administration once daily) is depicted in Figure 1. At the lowest dose tested (0.1 mg/

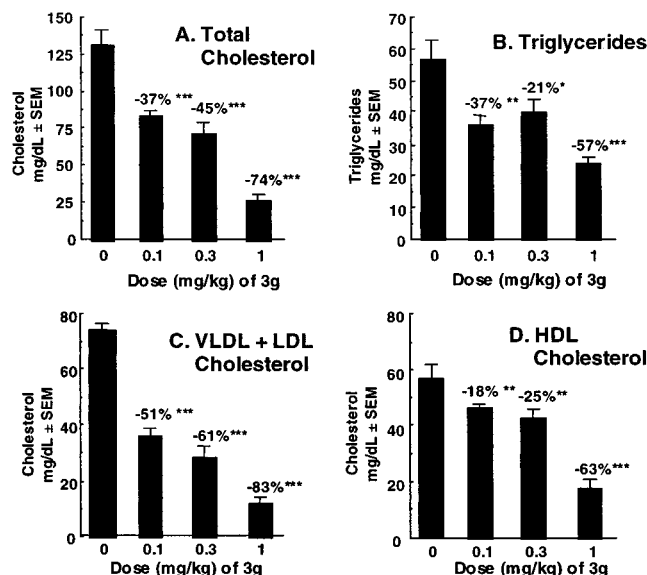


Figure 1. Effect of 3 days of treatment with **3g** on hamster plasma lipids. Golden Syrian hamsters were fed a standard diet (Purina 5001, which contains 0.02% TC and 4.5% TG) during the course of once daily oral treatment with **3g**. Fasting plasma lipid levels were determined 16 h after the last dose. The percent decreases were determined by comparing the lipid levels of drug-treated animals to those of the control-treated animals. Error bars indicate SEM; *p* values: * < 0.1, ** < 0.01, *** < 0.001.

kg), administration of **3g** resulted in a 37%, 37%, 51%, and 18% decrease in total cholesterol (TC), triglycerides (TG), VLDL/LDL, and HDL, respectively, as compared to vehicle controls. Significantly greater efficacy was observed at the highest dose tested (1 mg/kg). The HDL decrease was unlikely due to a direct effect on HDL production because the in vitro IC₅₀ for the inhibition of secretion of apolipoprotein AI with **3g** in HepG2 cells was found to be > 500 μM (highest concentration tested). No elevation of liver function tests (AST and ALT) were detected at any dose. An equally dramatic effect was observed in cynomolgus monkeys after once daily oral

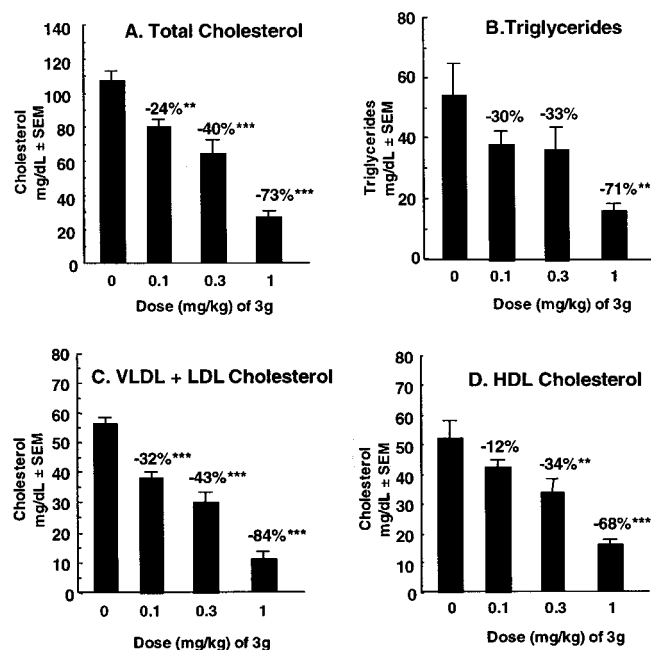


Figure 2. Plasma TC and TG concentrations in cynomolgus monkeys treated orally once daily with **3g** for 7 days. Fasting plasma lipid levels were measured 16 h after the last dose (0.1, 0.3, or 1 mg/kg/day) of **3g**. The percent decreases were determined by comparing the lipid levels of drug-treated animals to those of the control-treated animals. Error bars indicate SEM; *p* values: **<0.01, ***<0.001.

treatment for 7 days (Figure 2). At the highest dose tested (1 mg/kg), TC, TG, VLDL/LDL, and HDL were lowered 73%, 71%, 84%, and 68%, respectively. Tolerability was good in this study, but an approximate 2-fold increase in plasma ALT, AST, and CPK levels was observed. The significance on the modest increases in liver function enzymes in the monkey is unclear in light of the magnitude of the lipid-lowering response. Other hypolipemics, such as the statins, have shown a similar effect in humans.

To confirm the decrease in plasma lipids is due to an inhibition of lipoprotein production, as would be anticipated for an MTP inhibitor, a dose-response study of **3g** was performed in the fasted Triton rat assay, which measures the effect on hepatic apoB lipoprotein production.⁷ Intravenous injection of Triton WR1339, a non-ionic surfactant, has been shown to block the clearance of plasma TG-rich lipoproteins, enabling the measurement of their production in vivo. To ascertain the effects of MTP inhibition on TG secretion rates, Sprague-Dawley rats were fasted overnight for 18 h and orally dosed with **3g** 1 h before intravenous injection of Triton WR1339 (250 mg/kg). The secretion rate was determined by calculating the amount of TG accumulated during the first 2.5 h after the Triton injection. In this assay, **3g** was equipotent to **1** upon oral administration (ED_{50} = 0.15 mg/kg) but was nearly 4-fold more potent when given intravenously (ED_{50} = 0.04 mg/kg). At a dose of 1 mg/kg (po) and 0.3 mg/kg (iv), TG secretion rate was inhibited 94% and ~100%, respectively, thus demonstrating that **3g** is a potent inhibitor of hepatic lipoprotein production in vivo.

Based on the excellent in vivo profile of **3g** in models of lipid lowering, this compound was further evaluated for its pharmacokinetic properties. Standard pharmaco-

kinetic testing of **3g** in rats showed this compound possessed good oral bioavailability (81%) with a terminal elimination half-life of 4.8 h. In cynomolgus monkeys, oral bioavailability was somewhat reduced (23%) but half-life (6.9 h) was slightly greater.

Conclusion

We have demonstrated that the piperidine of BMS-201038 can be replaced by a benzimidazole ring system to provide a novel and highly potent class of MTP inhibitors. Molecular overlays indicate that the benzimidazole system provides a similar disposition of the flanking fluorenyl- and biphenylamide groups, suggesting that the heterocycle serves as a central scaffold. The enhanced potency of the benzimidazole-based inhibitors with small substituents at R and W suggests that orienting the biphenylamide at a position orthogonal to the central ring is desirable for optimal activity.

Currently, statin therapy is the first-line treatment for patients with hyperlipidemia and elevated cholesterol levels, although their effects on TG lowering is modest and variable. Preclinically, MTP inhibitors have dramatic effects not only on plasma cholesterol and LDL levels but on TG levels as well, offering the potential for greater efficacy and plasma lipid control in both hypertriglyceridemia and mixed hyperlipidemia. Compound **3g** has demonstrated superior potency both in vitro and especially in vivo as compared to the clinical agent BMS-201038. Indeed, it is the most potent MTP inhibitor described to date. On this basis, as well as its acceptable pharmacokinetic and safety profile, **3g** (BMS-212122) was brought forward for development as a potentially superior back-up agent to BMS-201038.

Experimental Section

All reactions were carried out under a static atmosphere of argon and stirred magnetically unless otherwise noted. All reagents used were of commercial quality and were obtained from Aldrich Chemical Co. or Sigma Chemical Co. Melting points were obtained on a Hoover Uni-melt melting point apparatus and are uncorrected. Infrared spectra were recorded on a Mattson Sirius 100-FTIR spectrophotometer. ¹H (400 Mz) and ¹³C (100 Mz) NMR spectra were recorded on a JEOL GSX400 spectrometer using Me₄Si as an internal standard. All flash chromatographic separations were performed using E. Merck silica gel 60 (particle size, 0.040–0.063 mm). Reactions were monitored by TLC using 0.25-mm E. Merck silica gel plates (60 F₂₅₄) and were visualized with UV light or 5% phosphomolybdic acid in 95% EtOH. BMS-201038 was synthesized at the Bristol-Myers Squibb Pharmaceutical Research Institute (Princeton, NJ).

5-Methyl-4-nitro-2,1,3-benzoselenadiazole (5). To a stirred solution of 48.95 g (0.40 mol) of **4** in 500 mL of 2.4 M hydrochloric acid at 80 °C under argon was added a warm solution of 88.77 g (0.80 mol) of selenium dioxide in 300 mL of water dropwise over the course of 30 min. After an additional 90 min, the reaction was cooled to room temperature and the solids were collected, washing with water. The brown solids were dried in vacuo at 50 °C to give the intermediate selenocycle (75.10 g) in 95% yield: TLC *R*_f 0.59 (CH₂Cl₂); mp 67–69 °C; ¹H NMR (DMSO-*d*₆) δ 2.39 (s, 3H), 7.35 (dd, 1H), 7.57 (s, 1H), 7.69 (d, 1H); ¹³C NMR (DMSO-*d*₆) δ 21.13, 120.96, 122.38, 132.54, 139.61, 158.72, 160.14. To a stirred solution of 72.00 g (0.365 mol) of the intermediate in 180 mL of 98% sulfuric acid at 10 °C was added a cold solution of 108 mL of 2:1 98% sulfuric acid/70% nitric acid over 1 h. The temperature of the reaction mixture was not allowed to rise above 20 °C. After an additional 60 min, the reaction was poured as a thin stream into 750 g of ice with rapid stirring. The fine yellow

slurry was filtered and the collected solids were washed five times with 200-mL portions of cold water. The moist cake was heated in 500 mL of ethanol to near boiling and then cooled to room temperature and the solid collected. Drying in vacuo at 50 °C gave **5** as a yellow solid (80.70 g) in 91% yield: TLC R_f 0.47 (CH_2Cl_2); mp 190–192 °C; ^1H NMR ($\text{DMSO}-d_6$) δ 2.46 (s, 3H), 7.62 (d, 1H), 8.01 (d, 1H); ^{13}C NMR ($\text{DMSO}-d_6$) δ 16.98, 125.44, 131.59, 131.88, 141.65, 150.59, 158.21. Anal. Calcd for $\text{C}_7\text{H}_5\text{N}_3\text{O}_2\text{Se}$: C, 34.73; H, 2.08; N, 17.36; Se, 32.61. Found: C, 34.96; H, 1.97; N, 17.35; Se, 32.59.

4-Methyl-3-nitro-1,2-benzenediamine (6, W = Me). To a stirred solution of hydriodic acid (25.0 mL, 57%, 189 mmol, stabilized with 1.5% hypophosphorous acid) at room temperature in argon was added 5.00 g (20.7 mmol) of **5**. The reaction vessel was placed in an oil bath preheated to 50 °C and the resulting deep red solution was vigorously stirred for 2 h. After cooling to room temperature the reaction mixture was poured into a stirred slurry of 24 g (0.2 mol) of sodium hydrogen sulfite in 50 mL of water. The resulting light yellow slurry was treated with an ice-cold solution of sodium hydroxide (7.5 g, 188 mmol) in 50 mL of water. Additional 6 M sodium hydroxide was added until the aqueous slurry was brought to pH 8. The resulting deep red slurry was filtered and the filtrate extracted three times with 200-mL portions of chloroform. The solids from the filtration were dissolved in 300 mL of chloroform and washed once with 50 mL of water. The organic extracts were combined, dried (Na_2SO_4) and evaporated to give **6** as a deep red solid (3.04 g) in 88% yield: TLC R_f 0.38 (1:49 $\text{Et}_2\text{O}:\text{CH}_2\text{Cl}_2$); mp 132–133 °C; ^1H NMR (CDCl_3) δ 2.38 (s, 3H), 3.35 (br s, 2H), 4.92 (br s, 2H), 6.49 (d, 1H), 6.74 (d, 1H); ^{13}C NMR (CDCl_3) δ 20.14, 120.11, 120.27, 125.71, 133.34, 133.46.

2,5-Dimethyl-4-nitro-1H-benzimidazole (7, W = R = Me). To a refluxing solution of 1.00 g (6.00 mmol) of **6** in 27 mL of ethanol and 7.2 mL of 5 M hydrochloric acid under argon was added 1.20 g (12.0 mmol) of 2,4-pentanedione over the course of 5 min. After an additional 60 min at reflux, the reaction was cooled and partially evaporated to remove ethanol. The residue was treated with saturated NaHCO_3 solution to pH 7, filtered, washed with water and dried in vacuo at 40 °C to give **7** ($\text{W} = \text{R} = \text{Me}$) as a tan solid (1.12 g) in 98% yield: TLC R_f 0.20 (EtOAc); mp 232–234 °C; ^1H NMR (CDCl_3) δ 2.70 (s, 3H), 2.83 (s, 3H), 7.19 (d, 1H), 7.84 (d, 1H); ^{13}C NMR (CDCl_3) δ 15.08, 22.13, 97.13, 104.91, 125.34, 126.26, 131.41, 152.68.

9-[4-(2,5-Dimethyl-4-nitro-1H-benzimidazol-1-yl)butyl]-N-(2,2,2-trifluoroethyl)-9H-fluorene-9-carboxamide (8, n = 1). To a solution of 9-fluorene-carboxylic acid (50 g, 240 mmol) in THF (1200 mL) at 0 °C was added dropwise a solution of *n*-butyllithium (2.5 M, 211 mL, 530 mmol) in THF. The yellow reaction was stirred at 0 °C for 1 h, then 1,4-dibromobutane (31.3 mL, 260 mmol) was added dropwise over 30 min. The reaction was stirred at 0 °C for 30 min, then warmed to room temperature for 30 h. The reaction was extracted with water (3 \times 750 mL). The combined aqueous layers were extracted with ethyl ether (800 mL). The aqueous layer was made acidic with HCl solution (1 N, 500 mL), then extracted with dichloromethane (3 \times 750 mL). The combined organic layers were dried over MgSO_4 . Evaporation gave the corresponding C-9 alkylated acid (71 g, 85%) as a white solid. To a solution of the intermediate acid (60 g, 173 mmol) and DMF (100 μL) in CH_2Cl_2 (600 mL) under argon at 0 °C was added oxalyl chloride (104 mL, 2.0 M in CH_2Cl_2 , 208 mmol) dropwise. The reaction was stirred at 0 °C for 10 min, then warmed to room temperature and stirred for 1.5 h. The reaction was concentrated in vacuo to give the crude acid chloride as a yellow oil. To a suspension of 2,2,2-trifluoroethylamine hydrochloride (25.9 g, 191 mmol) in CH_2Cl_2 (500 mL) at 0 °C under argon was added triethylamine (73 mL, 521 mmol) followed by dropwise addition of a solution of the crude acid chloride in CH_2Cl_2 (15 mL). The reaction was stirred at 0 °C for 1 h, diluted with CH_2Cl_2 (500 mL), and washed with water (2 \times 300 mL), 1 N HCl (2 \times 300 mL), saturated NaHCO_3 (2 \times 300 mL), and brine (2 \times 300 mL), then dried over MgSO_4 . Evaporation gave 80 g of a oil which was purified by flash chromatography on silica gel (2.5 kg). The crude product was loaded in a mixture of CH_2Cl_2 and hexane, and eluted with a

step gradient of 10% EtOAc /hexane (4 L) to 15% EtOAc /hexane (2 L) to 20% EtOAc /hexane (4 L). Pure fractions were combined and evaporated to give **8** ($n = 1$) (52.5 g, 71%) as a white solid: TLC R_f 0.32 (2:8 $\text{EtOAc}:\text{hexanes}$); mp 88–92 °C; ^1H NMR (CDCl_3) δ 0.83 (m, 2H), 1.68 (m, 2H), 2.42 (m, 2H), 3.21 (t, 2H), 3.68 (m, 2H), 5.36 (t, 1H), 7.36–7.59 (m, 6H), 7.78 (d, 2H); ^{13}C NMR (CDCl_3) δ 22.27, 32.70, 32.99, 40.65 (q), 62.17, 120.51, 124.07, 128.21, 128.71, 140.96, 144.88, 173.29.

9-[4-(2,5-Dimethyl-4-nitro-1H-benzimidazol-1-yl)butyl]-N-(2,2,2-trifluoroethyl)-9H-fluorene-9-carboxamide (9g, W = R = Me, n = 1). To a stirred slurry of 1.80 g (9.41 mmol) in 15 mL of DMF at room temperature under argon was added 1.75 g (33 mmol) of potassium carbonate. After 1 h, 4.26 g (10.0 mmol) of **7** was added and the reaction stirred for 86 h. The reaction mixture was quenched with 30 mL of water. The liquids were decanted away from the formed gummy solid, which was then washed with water. The semi-solid residue was triturated with 40 mL of ether. The resulting granular solid was chilled and filtered. The collected solid cake was washed with water, transferred to a round-bottom flask and evaporated from toluene. The dried residual solids were triturated with hot ethyl acetate and filtered to give 4.02 g of **9g** (80%) as a white solid: TLC R_f 0.20 (3:17 $\text{Et}_2\text{O}:\text{CH}_2\text{Cl}_2$); mp 181–183 °C; ^1H NMR (CDCl_3) δ 0.77 (m, 2H), 1.52 (m, 2H), 2.25 (s, 3H), 2.41 (m, 2H), 2.47 (s, 3H), 3.71 (m, 2H), 3.82 (t, 2H), 5.91 (t, 1H), 7.00 (d, 1H), 7.11 (d, 1H), 7.26 (t, 2H), 7.32 (t, 2H), 7.46 (d, 2H), 7.62 (d, 2H); ^{13}C NMR (CDCl_3) δ 13.20, 17.74, 20.94, 29.32, 35.49, 40.26 (q), 43.37, 61.65, 111.94, 119.94, 123.63 (q), 123.75, 124.00, 124.19, 127.72, 128.23, 134.84, 135.24, 139.61, 140.45, 144.42, 153.64, 172.86.

9-[4-(2,5-Dimethyl-4-amino-1H-benzimidazol-1-yl)butyl]-N-(2,2,2-trifluoroethyl)-9H-fluorene-9-carboxamide (10g, W = R = Me, n = 1). A stirred slurry of 1.05 g (1.96 mmol) of **9g** and 200 mg of 10% palladium-on-charcoal in 40 mL of ethanol was purged with argon and evacuated three times. Hydrogen was introduced to the partially evacuated solution via a balloon. After 14 h, the reaction mixture was purged with argon and passed through a 0.45- μm nylon filter, washing with dichloromethane. The filtrate was evaporated and then re-evaporated twice from dichloromethane to give **10g** as a white foam (0.958 g) in 99% yield: TLC R_f 0.13 (EtOAc); ^1H NMR (CDCl_3) δ 0.80 (m, 2H), 1.53 (m, 2H), 2.19 (s, 3H), 2.27 (s, 3H), 2.42 (m, 2H), 3.71 (m, 4H), 4.06 (br s, 2H), 5.66 (t, 1H), 6.40 (d, 1H), 6.82 (d, 1H), 7.40 (m, 4H), 7.48 (d, 2H), 7.69 (d, 2H); ^{13}C NMR (CDCl_3) δ 13.31, 16.41, 21.27, 29.46, 35.77, 40.49 (q), 43.32, 62.00, 98.31, 112.79, 120.30, 123.72 (q), 124.05, 124.48, 128.04, 128.54, 131.27, 133.77, 135.30, 140.76, 144.75, 148.62, 173.11.

9-[4-[2,5-Dimethyl-4-[[[4'-(trifluoromethyl)[1,1'-biphenyl]-2-yl]carbonyl]amino]-1H-benzimidazol-1-yl]butyl]-N-(2,2,2-trifluoroethyl)-9H-fluorene-9-carboxamide (3g). To a slurry of 1.72 g (6.47 mmol) of 4'-(trifluoromethyl)-2-biphenylcarboxylic acid (**11**, $\text{Z} = \text{OH}$), in 15 mL of dichloromethane at room temperature was added 0.85 mL (9.74 mmol) of oxalyl chloride followed by 75 μL of DMF. After 1 h, the resulting solution was evaporated and re-evaporated from dichloromethane. The residue was dissolved in 10 mL of dichloromethane and the solution was added dropwise to a solution of 3.21 g (6.34 mmol) of **10g** and 1.00 mL (7.17 mmol) of triethylamine in 15 mL of dichloromethane at room temperature. After 90 min, the reaction mixture was diluted with 100 mL of ethyl acetate and washed once with saturated sodium bicarbonate solution. The organic phase was dried (MgSO_4) and evaporated. Purification by flash chromatography on silica gel (5 \times 25-cm column, ethyl acetate) gave, after recrystallization from dichloromethane/hexanes, **3g** as a white crystalline solid (3.86 g) in 81% yield: TLC R_f 0.34 (EtOAc); mp 127–129 °C; ^1H NMR (CDCl_3) δ 0.81 (m, 2H), 1.56 (m, 2H), 2.26 (s, 3H), 2.36 (s, 3H), 2.42 (m, 2H), 3.69 (dq, 2H), 3.81 (t, 2H), 5.36 (t, 1H), 6.89 (d, 1H), 6.99 (d, 1H), 7.35 (m, 1H), 7.41 (m, 2H), 7.44 (m, 2H), 7.49 (d, 4H), 7.53 (dd, 1H), 7.59 (d, 1H), 7.69 (t, 3H), 7.75 (d, 2H), 7.85 (dd, 1H); ^{13}C NMR (CDCl_3) δ 13.53, 18.43, 21.35, 29.61, 35.76, 40.57 (q), 43.56, 62.02, 107.43, 120.44, 123.72 (d) 124.77, 124.92 (q), 124.99 (d) 125.24, 127.45,

128.00, 128.17, 128.71, 129.27, 129.34 (d), 130.25, 130.38, 136.14, 133.69, 136.14, 137.84, 138.95, 140.79, 144.03, 144.66, 150.66, 167.79, 173.12. Anal. Calcd for $C_{43}H_{36}F_6N_4O_2 \cdot CH_2Cl_2$: C, 63.46; H, 4.50; N, 6.58; F, 13.38. Found: C, 63.28; H, 4.30; N, 6.56; F, 13.10.

Supporting Information Available: Melting point and HRMS data for compounds **3a–g**, **5**, **6**, and **8**. This material is available free of charge via the Internet at <http://pubs.acs.org>.

References

- (1) Rosamond, W. D.; Chambless, L. E.; Folsom, A. R.; Cooper, L. S.; Conwill, D. E.; Clegg, L.; Wang, C.-H.; Heiss, G. Trends in the Incidence of Myocardial Infarction and in Mortality Due to Coronary Heart Disease, 1987 to 1994. *N. Engl. J. Med.* **1998**, *339*, 861–7.
- (2) Murray, C. J. L.; Lopez, A. D. Mortality by cause for eight regions of the world: Global Burden of Disease Study. *Lancet* **1997**, *349*, 1269–76.
- (3) Knopp, R. H. Drug Therapy: Drug Treatment of Lipid Disorders. *N. Engl. J. Med.* **1999**, *341*, 498–511.
- (4) Gordon, D. A.; Jamil, H. Progress towards understanding the role of microsomal triglyceride transfer protein in apolipoprotein-B lipoprotein assembly. *Biochim. Biophys. Acta* **2000**, *1486*, 72–83.
- (5) Wetterau, J. R.; Gregg, R. E.; Harrity, T. W.; Arbeen, C.; Cap, M.; Connolly, F.; Chu, C.-H.; George, R. J.; Gordon, D. A.; Jamil, H.; Jolibois, K. G.; Kunselman, L. K.; Lan, S.-J.; Maccagnan, T. J.; Ricci, B.; Yan, M.; Young, D.; Chen, Y.; Fryszman, O. M.; Logan, J. V. H.; Musial, C. L.; Poss, M. A.; Robl, J. A.; Simpkins, L. M.; Slusarchyk, W. A.; Sulsky, R.; Taunk, P.; Magnin, D. R.; Tino, J. A.; Lawrence, R. M.; Dickson, Jr., J. K.; Biller, S. A. An MTP inhibitor that normalizes atherogenic lipoprotein levels in WHHL rabbits. *Science* **1998**, *282*, 751–4.
- (6) Grivas, S.; Tian, W.; Ronne, E.; Lindstrom, S.; Olsson, K. Synthesis of mutagenic methyl- and phenyl-substituted 2-amino-3H-imidazo[4,5-f]quinoxalines via 2,1,3-benzoselenadiazoles. *Acta Chem. Scand.* **1993**, *47*, 521–8.
- (7) Serougne, C.; Mathe, D.; Ferezou, J.; Bertin, C.; Riottot, M.; Lutton, C.; Jacotot, B. J. Hypercholesterolemia induced by cholesterol- or cystine-enriched diets is characterized by different plasma lipoprotein and apolipoprotein concentrations in rats. *J. Clin. Biochem. Nutr.* **1995**, *18*, 55–64.

JM000494A